Available online at www.sciencedirect.com
SCIENCE DIRECT®
Journal of Power Sources 119–121 (2003) 938–942
JOURNAL OF POWER SOURCES
www.elsevier.com/locate/jpowsour

Li_2CuO_2 as an additive for capacity enhancement of lithium ion cells

G. Vitins, E.A. Raekelboom, M.T. Weller, J.R. Owen*

Department of Chemistry, University of Southampton, Highfield, Southampton SO17 1BJ, UK

Abstract

The lithium-rich cuprate Li_2CuO_2 shows a high specific charge capacity of 320–340 mAh g^{-1} due to lithium extraction on oxidation up to 4.5 V versus Li. However, poor reversibility of this reaction limits the application of this material in lithium ion cells as the active material in the positive electrode. Nevertheless, this inexpensive, easily synthesised, air stable material may be useful as an additive to the positive electrode for reduction of capacity loss caused by poor reversibility of the negative electrode. Electrochemical testing of a composite Li_2CuO_2/$LiMn_2O_4$ electrode versus Li shows that no interference occurs between these two materials and that $LiMn_2O_4$ maintains its long cycle life in the voltage range 3.0–4.5 V versus Li. The calculated enhancement of effective specific capacity due to the additive increases with the fraction of charge lost at the negative, reaching 10% enhancement at 20% capacity loss.

Keywords: Lithium cuprate (Li_2CuO_2); Lithium manganese oxide ($LiMn_2O_4$); Composite electrodes; Lithium cells; Lithium ion cells

1. Introduction

A common problem in lithium ion batteries is a loss of the specific capacity when a passivation layer forms on the negative electrode and a fraction of lithium, extracted from the positive electrode, is bound irreversibly on the negative electrode in the initial charge of the cell. A complex passivation film of electrolyte reduction products is formed on the electrode surface [1–3]. This effect is well documented for carbon electrodes where the extent of irreversible capacity depends on the composition of the electrolyte and the type of carbon. Many efforts have been made to minimise the irreversible capacity and stabilise the surface of the carbon-based negative electrodes which are normally used in commercial lithium ion systems at present. Particularly, a high coulombic efficiency has been achieved using electrolytes with ethylene carbonate, which significantly increases the stability of the passivation film [1,2].

A way to balance the charge capacity of both electrodes and to increase the overall specific capacity of lithium ion cells was proposed by West et al. [4]. A material with a high initial charge capacity can be used in order to balance the fraction of the irreversible capacity. Good reversibility is not a necessity, but the additive must not impair the performance of the base material. Particularly, they have suggested lithium-rich manganese oxide $Li_2Mn_2O_4$ and $Li_2Co_{0.4}Mn_{1.6}O_4$ [4,5] as additives, exhibiting up to 270 mAh g^{-1} in the initial charge to 4.5 V versus Li. AMO_2 (A = Na, Li; M = Mn, Fe) were also suggested as materials which can maintain electrochemical activity on repeated cycling. However, all of the above compounds are rather difficult to prepare and unstable in moist air.

In this paper, we analyse the electrode performance of Li_2CuO_2, both pure and a mechanically mixed composite with $LiMn_2O_4$ in lithium cells. This lithium cuprate is particularly lithium-rich, can be synthesised by a simple solid state synthesis [6,7], and is air stable. This work was carried out to investigate its performance as an charge balancing additive in positive electrodes. (After we finished our studies we found that this material was included in a patent [8] for application as an additive in positive electrodes.)

2. Experimental

Li_2CuO_2 was prepared by reacting corresponding amounts of $LiOH{\cdot}H_2O$ and CuO in air in an alumina crucible. Two different heat treatments were used. The first sample was heated at 800 °C for 15 h. The second sample was treated at 410 °C for 2 days and an intermediate regrinding was used. The purity of product powders was

* Corresponding author. Tel.: +44-2380-592184; fax: +44-2380-593781.
E-mail address: jro@soton.ac.uk (J.R. Owen).

0378-7753/03/$ – see front matter © 2003 Elsevier Science B.V. All rights reserved.
doi:10.1016/S0378-7753(03)00236-2

measured by X-ray powder diffraction using a Siemens D5000 diffractometer with Cu $K\alpha_1$ radiation. An optimised material in the $LiMn_2O_4$ group, $Li_{1.05}Mn_2O_{4.12}$ (Sedema, Belgium) was used as a base electrode material in composite electrodes with Li_2CuO_2. This $LiMn_2O_4$ has a capacity of 120 mAh g^{-1} and a quite stable cycle life at the 4 V plateau. Thus it can also be used as a good reference material.

Spring-loaded cell holders made of stainless steel [9,10] were used in two-electrode electrochemical testing. Positive electrodes comprised 75 wt.% of active material, 20 wt.% of acetylene black (100% compressed, Chevron) and 5 wt.% of PTFE. The components were mixed and compressed together in a rolling mill. The thickness of the electrode films was around 130–160 μm. The surface area of projection of electrode discs made from the film was 1 cm^2. Typically, the weight of active material in positive electrodes was around 15–17 mg. The composite electrodes were dried in vacuum at 120 °C in a Büchi tube furnace and then transferred to the Ar-glove box, where cells were finally assembled. A Perkin-Elmer, Bio-Logic Science Instruments VMP was used as a galvanostat for constant current cycling. Lithium metal was simultaneously used as a reference and counter electrode. A glass fibber separator (Whatman) soaked with 1 M $LiPF_6$ in propylene carbonate electrolyte (Merck) separated the positive and negative electrodes.

3. Results and discussion

Powder X-ray diffraction confirmed that the main product of synthesis in both heat treatments at 410 and 800 °C is the orthorhombic Li_2CuO_2. Traces of CuO were seen in the powder made at 410 °C. It can be concluded that reacting species have a moderately high reactivity and mobility, which allow for a low temperature synthesis with a quite short reaction time. The low melting point of LiOH at 450 °C probably aids impregnation of CuO powder with Li^+ ions, thereby reducing the diffusion distance required for the reaction. In this paper, we present results obtained with the material prepared at 800 °C.

The charge–discharge curve for Li_2CuO_2 of Fig. 1 shows that on an initial lithium extraction at C/16 (or 0.204 mA cm^{-2}; 11 mA g^{-1}) the material showed a capacity of 320 mAh g^{-1}. During this first charge the cell voltage quickly increased from the open circuit potential of 2.9–3.8 V and then decreased to ca. 3.3 V. Such behaviour is normally attributed to the nucleation energy of a second phase. The coexistence of Li_2CuO_2 and $LiCuO_2$ at this stage was confirmed by our X-ray diffraction studies in agreement with the work of Arai et al. [11]. The capacity of this plateau fits well with the 243 mAh g^{-1} needed to remove one lithium from the structure, forming Cu^{3+} according to reaction 1(a). Further oxidation at the 4.1 V plateau proceeds with irreversible decomposition of the material according to reaction 1(b) as confirmed by our X-ray phase analysis and the studies by Arai et al [11]:

$$Li_2CuO_2 \rightarrow LiCuO_2 + Li^+ + e^- \quad 1(a)$$

$$2LiCuO_2 \rightarrow 2Li^+ + 2e^- + 2CuO + O_2 \quad 1(b)$$

Comparison of the observed 320 mAh g^{-1} end point with 486 mAh g^{-1} expected for reaction 1 shows that not all the material is decomposed to CuO/O_2. Reaction 1(b) is hindered, possibly by formation of CuO on surface of particles. On the following insertion reaction down to 1.8 V versus Li a capacity of 240 mAh g^{-1} is regained between 2.9 and 2.0 V. Again X-ray phase studies have confirmed reappearance of the two phases $LiCuO_2$ and Li_2CuO_2 together with CuO, which cannot be reduced until below 2 V versus Li [12].

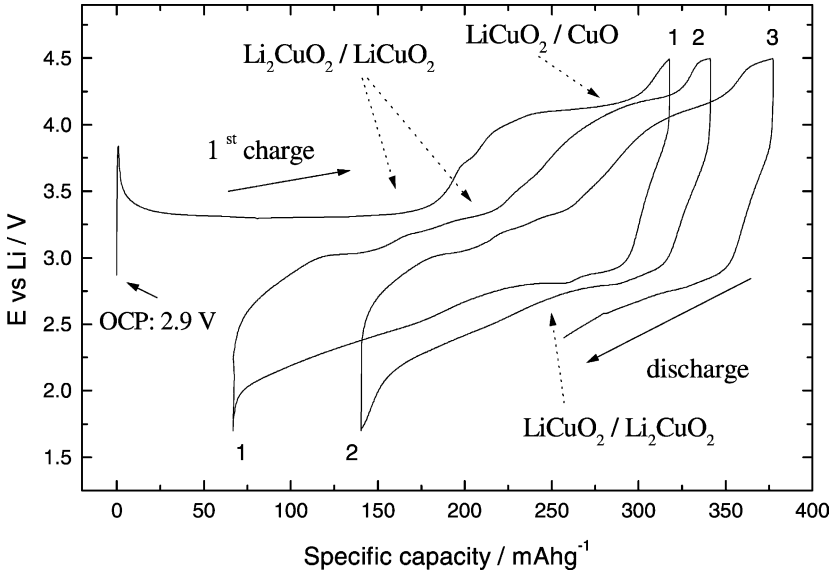

Fig. 1. Charge–discharge curves for the Li_2CuO_2 electrode cycled in voltage range 1.8–4.5 V at a specific current 11 mA g^{-1} (1 Li/26 h in Li_xCuO_2).

On the following cycles the material loses capacity rapidly, and the charge–discharge curves proceed with a large hysteresis of ca. 1–1.5 V despite the very slow rate used. The hysteresis can be ascribed to kinetically hindered structural transitions occurring during the oxidation and reduction of Li_xCuO_2. The phase transition Li_2CuO_2–$LiCuO_2$–CuO involves not only slow lithium ion transport but also changes in its coordination from tetrahedral in $LiCuO_2$ to octahedral in Li_2CuO_2. It must also involve significant shifts of $Cu^{2+/3+}$ ions; although both phases are similar having infinite chains of edge-sharing CuO_4 planes, they still have a different arrangement respectively in the lattice. The structural difference is also accompanied by a significant variation in Li_xCuO_2 density from 3.7 to 4.5 g cm^{-3} for Li_2CuO_2 and $LiCuO_2$, respectively.

In contrast with the results of Arai et al. [11] where a maximum charge capacity of ca. 480 mAh g^{-1} was gained in a slow charge of Li_2CuO_2 to 4.3 V, our experiments showed a maximum charge capacity of 340 g cm^{-3} for Li_2CuO_2 prepared at 410 °C. We also did not observe the appearance of mixed valence cuprate $Li_{1.5}CuO_2$ on extraction as reported in [11]. The reason for this can be the difference in electrode equilibration times prior the X-ray diffraction. $Li_{1.5}CuO_2$ is unstable at above 300 °C at normal pressure [13], and as a pure phase it can be obtained only in extreme synthesis conditions, e.g. at high oxygen pressure or under hydrothermal conditions [14–16]. Similarly, $LiCuO_2$ can only be prepared by chemical delithiation from Li_2CuO_2 or $Li_{1.5}CuO_2$ [12,17,18].

Examples of the performance of a composite electrode, consisting of 79.5 wt.% of $LiMn_2O_4$ (120 mAh g^{-1}) and 20.5 wt.% of Li_2CuO_2 (320 mAh g^{-1} in the first charge only), are shown in Figs. 2 and 3. In the initial charge, the electrode delivers 162 mAh g^{-1} as expected considering the capacity of pure oxide components. The initial overpotential and the 3.3 V plateau are characteristic of the

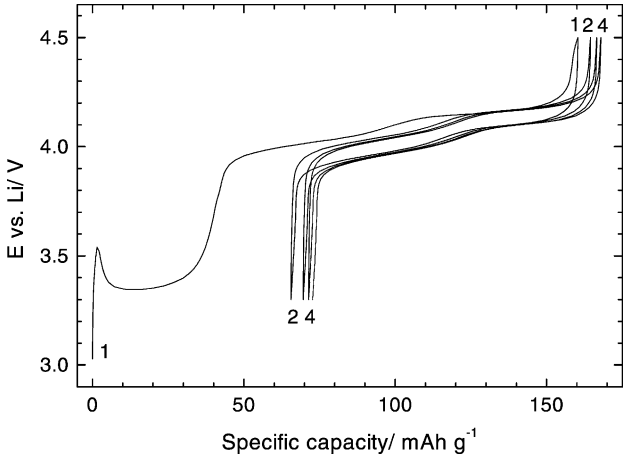

Fig. 2. Charge–discharge curves for composite electrode, comprising 79.5% $LiMn_2O_4$ (120 mAh g^{-1}) and 20.5% Li_2CuO_2 (320 mAh g^{-1}) as an active material, cycled in voltage range 3.3–4.5 V. The current density in the first charge is 12 mA g^{-1}, then 39 mA g^{-1}.

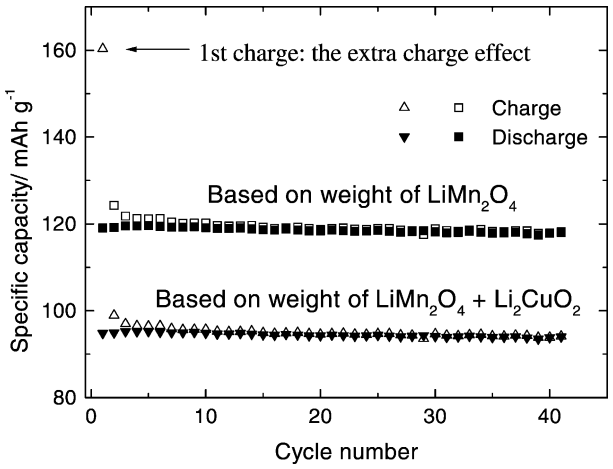

Fig. 3. Specific capacity vs. cycle number for composite comprising 79.5% $LiMn_2O_4$ (120 mAh g^{-1}) and 20.5% Li_2CuO_2 (320 mAh g^{-1}) cycled in voltage range 3.3–4.5 V. The current density in the first charge is 12 mA g^{-1} then 39 mA g^{-1}.

oxidation of Li_2CuO_2. The 4 V plateau is also extended, as Li_xCuO_2 is being oxidised and partly decomposed into CuO and O_2 as suggested above. On the following cycles the electrode has lost 41% of charge capacity and the reversible capacity remains at 95 mAh g^{-1}, as only $LiMn_2O_4$ is active in range 3.3–4.5 V versus Li. However, all the capacity loss may be ascribed to the additive and we may conclude that the additive has no detrimental effect on the $LiMn_2O_4$ active material.

In this experiment, no advantage of the additive is seen for the cycling of the composite electrode in a wide voltage range 1.8–4.5 V (Fig. 4). The capacity fades rapidly from the maximum at 270 mAh g^{-1} down to 215 mAh g^{-1} for pure $LiMn_2O_4$ and 185 mAh g^{-1} with the Li_2CuO_2 addition at the 14th cycle. The addition of Li_2CuO_2 also increases hysteresis in the voltage profile.

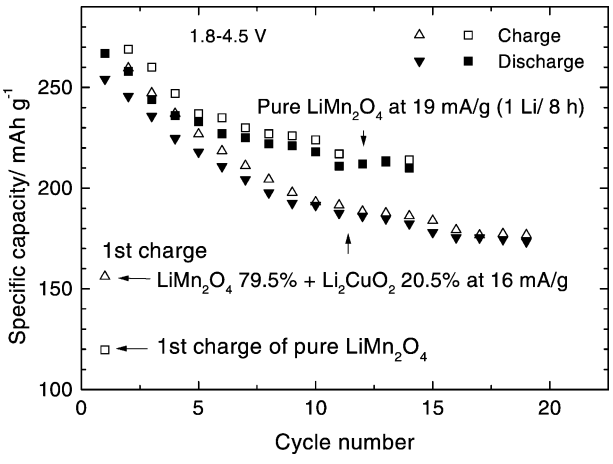

Fig. 4. Specific capacity vs. cycle number for composite comprising 79.5% $LiMn_2O_4$ (120 mAh g^{-1}) and 20.5% Li_2CuO_2 (320 mAh g^{-1}) cycled in voltage range 1.8–4.5 V. The current density is of 16 mA g^{-1}. Note that the initial charge starts at the open circuit voltage of 3 V vs. Li.

The benefits of adding Li_2CuO_2 to $LiMn_2O_4$ can only be appreciated when the positive electrode is used in conjunction with a partially-reversible negative electrode such as carbon. In that case the effective capacity of the positive electrode is decreased according to the amount of lithium consumed irreversibly at the negative electrode. The following calculation shows the amount of capacity decrease for a perfectly reversible positive electrode can be limited by the addition of a non-reversible, primary, material of higher specific capacity. It is applicable to the case of $LiMn_2O_4$/carbon because any irreversible capacity loss in $LiMn_2O_4$ is negligible compared with that observed on the first cycle with a carbon negative.

The reversible specific capacity and specific capacity loss at the negative electrode are denoted Q_{rev} and Q_{irrev}, respectively. Both of these contribute to the total specific capacity of the negative, Q_{neg} during the first charge:

$$Q_{neg} = Q_{rev} + Q_{irrev}$$

The optimum amount of a fully-reversible positive electrode material in a cell is that which provides a charge equal to $(Q_{rev} + Q_{irrev})$ per unit mass of negative electrode. However, the reversible charge passed per cycle after the first is only Q_{rev}. Accordingly, the effective charge available from the positive electrode is reduced according to Eq. (2):

$$Q_{pos}{}' = Q_{pos,N=1}\left(\frac{Q_{rev}}{Q_{rev} + Q_{irrev}}\right) = Q_{pos,N=1}(1-f) \qquad (2)$$

where Q_{pos} is the nominal specific capacity of the positive electrode. $Q_{pos}{}'$ represents the effective specific capacity of the positive electrode on discharge and subsequent cycles and f is the fractional capacity loss at the negative, $Q_{irrev}/(Q_{rev} + Q_{irrev})$.

The purpose of the additive is to provide the charge required to compensate for Q_{irrev}, while the normal positive electrode material supplies charge for Q_{rev}. The masses of each material are therefore as follows:

$$\frac{m_{pos}}{m_{neg}} = \frac{Q_{rev}}{Q_{pos}}; \quad \frac{m_{add}}{m_{neg}} = \frac{Q_{irrev}}{Q_{add}}; \quad \frac{m_{pos} + m_{neg}}{m_{neg}} = \frac{Q_{rev}}{Q_{pos}} + \frac{Q_{irrev}}{Q_{add}} \qquad (3)$$

The reversible charge produced is just Q_{rev}, and therefore the effective specific charge of the composite positive electrode, Q_{eff} is given in Eq. (4):

$$Q_{eff} = \frac{Q_{rev}}{(Q_{rev}/Q_{pos}) + (Q_{irrev}/Q_{add})} \qquad (4)$$

Replacing the terms Q_{rev} and Q_{irrev} by $(1-f)Q_{neg}$ and fQ_{neg}, respectively, we obtain Eq. (5):

$$Q_{eff} = \frac{1-f}{(1-f/Q_{pos}) + (f/Q_{add})}$$
$$Q_{eff} = \frac{(1-f)Q_{pos}}{(1-f(1-Q_{pos}/Q_{add}))} \qquad (5)$$

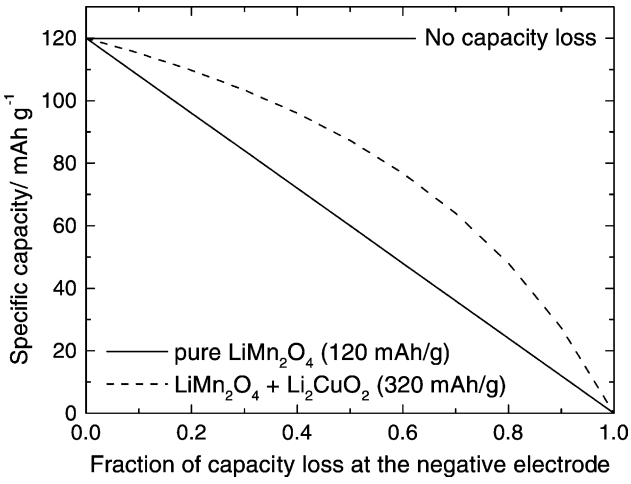

Fig. 5. Calculated effective specific capacity of the active material in the positive electrode of an optimised cell vs. the fraction of capacity loss at the negative electrode. The capacities of the positive and negative electrodes are assumed to be balanced in the first charge of the lithium ion cell.

The expression shown in Eq. (5) has been calculated as a function of f for fixed values of $Q_{pos} = 120$ mAh g^{-1} and $Q_{add} = 320$ mAh g^{-1} and is shown in Fig. 5. The result shows a 10% enhancement of specific capacity when coupled with a negative electrode with 20% capacity loss. In general there is a significant improvement in the effective specific capacity for a wide range of values of the capacity loss at the negative.

4. Conclusions

1. The lithium-rich cuprate, Li_2CuO_2 shows poor reversibility due to slow ion transport and a range of non-topotactic transitions of the lattice during cycling.
2. However, it delivers high capacity of ca. 320 mAh g^{-1} in the first charge, which can be successfully used in order to reduce the charge loss effect in lithium ion cells by more than 10%.
3. Li_2CuO_2 is easy and inexpensive to prepare. It can be prepared at low temperature, e.g. 410 °C in air. In this respect it appears to be superior to most of AMO_2 compounds, which have capacities below 280 mAh g^{-1} and are often difficult to prepare.

References

[1] J.R. Dahn, et al., in: G. Pistoia (Ed.), Lithium Batteries, Industrial Chemistry Library, Elsevier, Amsterdam, 1994, pp. 22–28.
[2] B. Simon, J.P. Boeuve, J. Power Sources 43–44 (1993) 65.
[3] Y. Ein-Eli, B. Markovsky, D. Aurbach, Y. Carmeli, H. Yamin, S. Luski, Electrochim. Acta 39 (1994) 255.
[4] K. West, G. Vitins, R. Koksbang, Electrochim. Acta 45 (2000) 3141.
[5] R. Koksbang, K. West, A.S. Danionics, G. Vitins, Patent 18.11.1999, WO9959214.
[6] R. Hoppe, H. Rieck, Z. Anorg. Allg. Chem. 379 (1970) 157.
[7] F. Sapiña, J. Rodrígeuez-Carvajal, M.J. Sanchis, R. Ibáñez, A. Beltrán, D. Beltrán, Solid State Commun. 74 (1990) 779.

[8] J. Barker, M.Y. Saidi, Valence Technology Inc., Patent 28.04.1998, US5744265.
[9] S. Skaarup, Design and interpretation of cycling experiments on solid state batteries, in: B.V.R. Chowdari, S. Radhakrishna (Eds.), Proceedings of the International Symposium on Solid State Ionic Devices, Singapore, 1988, pp. 35–53.
[10] T. Le Gall, K.H. Reiman, M.C. Grossel, J.R. Owen, J. Power Sources 119–121 (2003) 316–320.
[11] H. Arai, S. Okada, Y. Sakurai, J. Yamaki, Solid State Ionics 106 (1998) 45.
[12] N.A. Godshall, Solid State Ionics 18–19 (1986) 788.
[13] W. Klemm, G. Wehrmeyer, H. Bade, Z. Electrochem., Ber. Bunsenges. Phys. Chem. 63 (1956) 56.
[14] M.T. Weller, D.R. Lines, D.B. Currie, J. Chem. Soc., Dalton Trans. (1991) 3137.
[15] D.B. Currie, M.T. Weller, J. Mater. Chem. 3 (1993) 229.
[16] E.A. Raekelboom, A.L. Hector, M.T. Weller, J.R. Owen, J. Power Sources 97–98 (2001) 465.
[17] R. Berger, L.-E. Tergenius, J. Alloys Compd. 203 (1994) 203.
[18] K. Imai, M. Koike, H. Takei, H. Sawa, D. Shiomi, K. Nozawa, M. Kinoshita, J. Phys. Soc. Jpn. 61 (1992) 1819.